Acceleration signatures in the dayside boundary layer and the cusp

M. Yamauchi[1], L. Andersson[1], P.-A. Lindqvist[2], S. Ohtani[3], J. Clemmons[4], J.-E. Wahlund[5], L. Eliasson[1], and R. Lundin[1]

[1]Swedish Institute of Space Physics, Box 812, S-98128 Kiruna, Sweden
[2]Alfven Lab., KTH, SE-10044 Stockholm, Sweden
[3]JHU/APL, Laurel, MD 20723-6099, USA
[4]Aerospace Corp., Los Angeles, CA 90009, USA
[5]Swedish Institute of Space Physics, SE-75591 Uppsala, Sweden

Camera-ready Copy for

Physics and Chemistry of the Earth

Manuscript-No. 09-01

Offset requests to:
M. Yamauchi

Acceleration signatures in the dayside boundary layer and the cusp

M. Yamauchi[1], L. Andersson[1], P.-A. Lindqvist[2], S. Ohtani[3], J. Clemmons[4], J.-E. Wahlund[5], L. Eliasson[1], and R. Lundin[1]

[1]Swedish Institute of Space Physics, Box 812, S-98128 Kiruna, Sweden
[2]Alfven Lab., KTH, SE-10044 Stockholm, Sweden
[3]JHU/APL, Laurel, MD 20723-6099, USA
[4]Aerospace Corp., Los Angeles, CA 90009, USA
[5]Swedish Institute of Space Physics, SE-75591 Uppsala, Sweden

Received 1999-12-21 – Revised 2000-05-23 – Accepted 2000-06-30

Abstract. Freja data show various electron acceleration signatures in the cusp and the dayside boundary layer: (1) time dispersive super-Alfvénic electrons followed by strong wave activity which accompanies transient downward super-thermal electron burst in both the boundary layer and the cusp; (2) quasi-stationary bi-directional electron burst coinciding with localized intense field-aligned current in the boundary layer; (3) downgoing electron burst without visible time dispersion in the cusp; and (4) thermal electrons accelerated by electrostatic potential in both the boundary layer and the cusp. The first and last signatures are different between two regions for typical energies and fluxes, and these differences probably reflect the different auroral emission in the cusp proper (red) and the boundary layer (green). Contributions of these electrons to the large-scale field-aligned currents are also different between two regions. The dispersed electron burst is probably accelerated within 1 Re above the ionosphere. From this result we believe that the cusp red aurora is caused mainly by accelerated electrons, but not by the smoothly entering magnetosheath electrons without acceleration. This also requires revisions of flux transfer event models for the structured cusp red aurora.

Phys. Chem. Earth, 26, 195-200, 2001.
doi:10.1016/S1464-1917(00)00107-0
Published by Elsevier Ltd.
www.irf.se/∼yamau/papers/yamauchi2001_figures/

1 Introduction

The cusp red aurorae (630 nm wavelength from oxygen atoms), both non-structured one during weak interplanetary magnetic field (IMF) and structured one during southward IMF (e.g., Sandholt et al., 1998; Yamauchi et al., 1995), have long been assumed as the signature of the simple penetration of the magnetosheath electrons with about 100 eV temperature. However, these thermal electrons are not as important as the electrostatically accelerated electrons or bursty electrons in generating the cusp red aurora during southward IMF (Yamauchi, presentation at NATO workshop in Longyearbyen, 1997; Pfaff et al., 1998). Both types of electrons have characteristic energies of a few hundred eV, corresponding to red (630 nm) auroral emission. Here we call "burst" if very intense downgoing (or upgoing or bi-directional) electrons with wide energy spectrum from 40 eV (lowest energy limit of Freja electron spectrometer) to sometimes up to several keV are detected very locally (< 5 km).

The downgoing bursty electrons mostly have super-thermal velocities, and are most likely accelerated by the kinetic/inertia Alfvén waves within 1 Re distance from the ionosphere, according to satellite particle (proton and electron), field (electric and magnetic), and wave observations (Pfaff et al., 1998; see also Chaston et al., 1999). Both the bursty acceleration signature and the electrostatic acceleration signature are similar between in the cusp-cleft region and in the auroral oval (Pfaff et al., 1998; Lundin and Eliasson, 1991).

Thus even inside the cusp, the electrons are accelerated just above the ionosphere. These electrons are less energetic than the accelerated electrons in boundary layer, causing a difference in color (red oxygen line for the cusp and green oxygen line for the boundary layer). This fact requires revisions of interpretations of the cusp phenomena observed from ground (optical and radar observations). The structures in the cusp red aurora must reflect those acceleration mechanisms there, and the midday poleward moving auroral forms do not necessarily reflect the magnetopause structure such as the flux transfer events.

We now have to know the differences of electron acceleration between the boundary layer (BPS of Winningham et al. (1975)) and the cusp. Aside characteristic

Correspondence to: M. Yamauchi

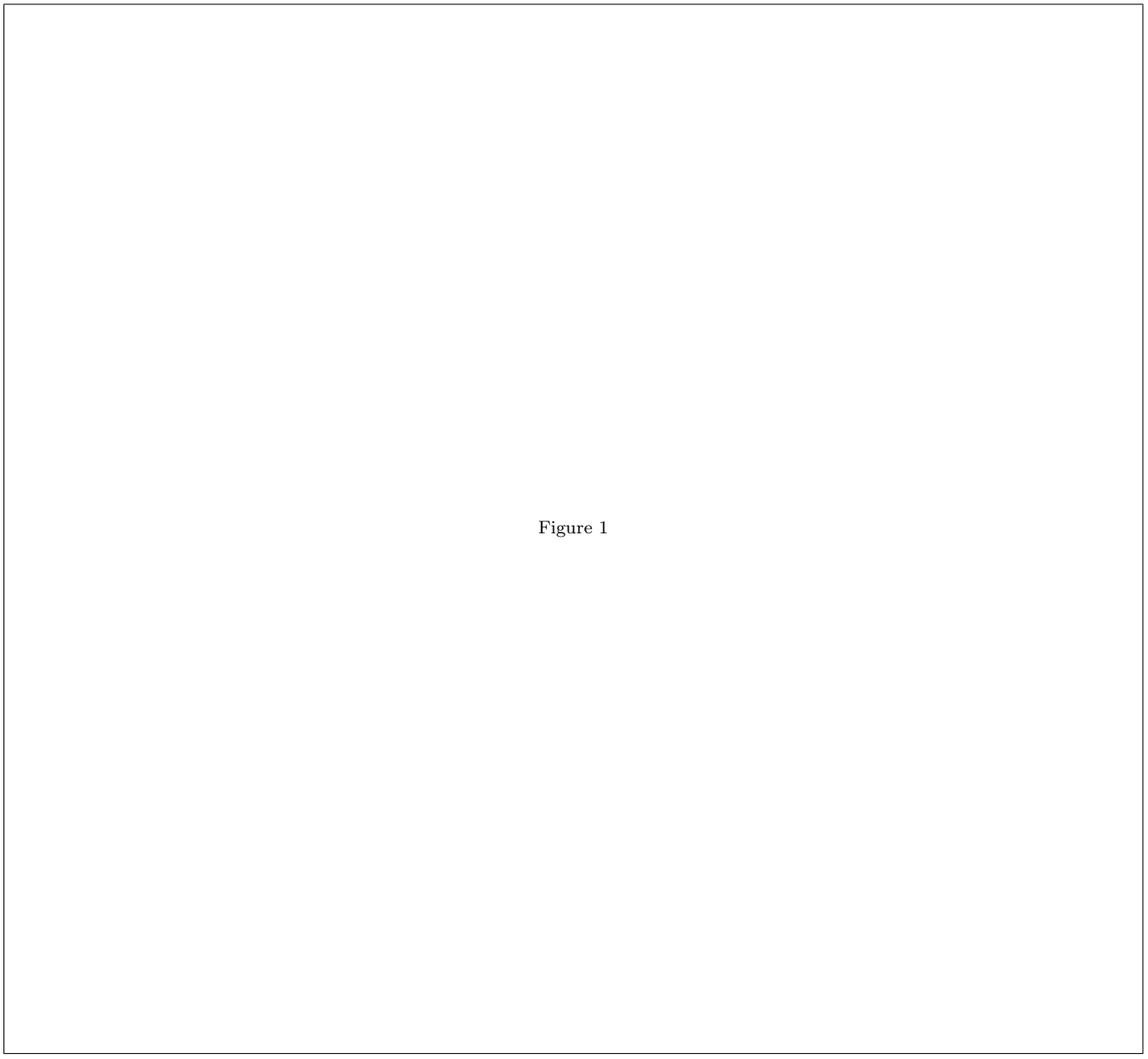

Fig. 1. Freja particle and field data for orbit 5396 (1993-11-18). From the top to bottom: northward (ΔB_n) and eastward (ΔB_e) magnetic deviation (subtracted by the model field), energy-time spectrograms of heavy ions (mainly oxygen), light ions (mainly proton), and electrons, and parallel and eastward electric fields. The electric field data has non-zero offset due to the satellite attitude problem, but yet we can use its slope and spikes.

energy, there is a qualitative difference between the cusp electrons and the boundary layer electrons in contributions to large-scale field aligned currents (FACs). The majority of the morning region 1 (R-1) FAC in the auroral oval region is composed of a few narrow sheets of intense downward FACs associated with narrow but and intense electron bursts, whereas the cusp region 1 (C-1) or region 0 (C-0) FAC (name after Yamauchi et al. (2000)) is not a simple summation of small- or meso-scale FACs although many meso-scale monopolar magnetic signatures (i.e., pairs of upward and downward FACs) are seen inside the cusp (Potemra et al., 1987; Yamauchi et al., 2000). They seem to reflect the meso-scale magnetic field oscillation inside the cusp without contributing to the large-scale FACs.

Figure 1 shows one such example (Freja orbit 5396) used in Yamauchi et al. (2000). Please refer to this paper for naming of regions etc. The particle data show structured BPS-like electrons (Winningham et al., 1975) up to 1435:20 UT and dense plasma injection in the cusp proper at 1439:50-1443:40 UT. The eastward component of the magnetic deviation (ΔB_e) shows large slopes in both the BPS-like region and the boundaries of the cusp proper, and they correspond to R-1 (1434:40-1435:25 UT; downward), C-0 and C-1 FACs (1440:00-1441:10 UT; downward, and 1442:40-1443:45 UT; upward). The northward component of the magnetic deviation (ΔB_n) is smaller than ΔB_e except for some meso-scale bipolar signatures inside the cusp.

The figure apparently shows that the auroral oval FAC (R-1) in BPS is composed of steps of sharp increase of ΔB_e (i.e., intense downward FAC sheets) associated with the electron bursts at 1434:42 UT (+400 nT jump), at 1435:11 (+50 nT jump) and at 1435:25 UT (+50 nT jump). On the contrary, C-0 FAC at 1440:00-1441:10 UT is composed of many large slopes of ΔB_e (but not as sharp as the R-1 FAC case), and a wide region contributes to this large-scale FAC. Contrary to R-1 case, these changes in ΔB_e (even the largest one) do not accompany the strong electron burst in the cusp. One may also notice a large meso-scale monopolar signature of ΔB_n (localized pairs of up and down FACs, e.g., at 1441:10 UT) inside the cusp, but they do not constitute the large-scale FACs. Then ΔB_e at the boundary of the cusp is better understood as a wide slope with many embedded bipolar signatures rather than as a summation of steps as is the case with auroral oval FAC. The same result was obtained with Viking data (Yamauchi et al., 1998).

The above finding raised further questions on the difference between the cusp (C-1/C-0 FACs) and BPS (R-1 FAC). (1) Is morphology of the electron burst always the same in each region (the cusp and BPS)? (2) Is role of the electron burst always the same in each region? (3) How about the electrostatic potential structure in various dayside regions? (4) How much of these differences originates from the travelling distance (e.g., growth of instabilities and plasma loss rate), from the injection mechanisms, or from the co-existing particle population (e.g., conditions for instabilities)? (5) What is the relation between these particle signatures and optical (aurora) signatures? We study some of these questions in this paper by examining the micro-scale structure of the dayside electron bursts, first in the morningside boundary layer and then in the cusp.

Figure 2

Fig. 2. Electron spectrogram with 62 ms (= about 450 m) resolution at around 1435:10 UT of Figure 1. The differential energy flux is given in $eVcm^2s^{-1}eV^{-1}str^{-1}$. Pitch angles (PA) of the measurements are listed in each panel. From top to bottom: nearly field-aligned downgoing electrons, obliquely downgoing electrons, nearly perpendicular electrons, and obliquely upgoing electrons (yet inside loss cone at Freja altitude). Numbers $(1, 2, 3, \cdots 10)$ at top and bottom sides are time tags used in the text.

2 Observations of Electron Acceleration

Figures 2-4 show the highest time-resolution data (every 62 ms or about 450m horizontal distance) from Figure 1 for the bursty electrons: Figure 2 at 1435:10 UT in BPS, Figure 3 at 1434:40 UT in BPS, and Figure 4 at 1440:27 UT in the cusp-cleft.

2.1 Boundary Layer

The first example at 1435:10 UT shows clear energy-time dispersion (time-3 to time-7 in Figure 2) followed

by a burst of sub-keV electrons (time-8 and time 9) in the downgoing direction as if the burst part arrived together with a travelling wave. Since 100 eV electron travels about 6000 km/s which is similar to the local Alfvén speed (Lysak, 1997), this wave is most likely the Alfvén wave, and the downgoing electrons arriving before time-8 became free from this Alfvén wave some time earlier. These "free" electrons may constitute time-of-flight dispersion. Electrons arriving together with the wave are yet faster than the thermal velocity, and hence we call this phenomenon the super-thermal electron burst (STEB).

The AC electric and magnetic fields in Figure 1 show high-amplitude disturbances at exactly the time of the electron burst, and one-second resolution DC magnetic field data show a downward FAC for about several seconds including the time of this electron event. The electron flux during the other period of this several seconds (inside FAC sheet) is very low compared to the burst. The high-resolution field data (not shown here) actually demonstrate a signature of the Alfvén wave at this time with $\delta E_\perp/\delta\Delta B_\perp$ amplitude ratio $\sim$ local Alfvén wave velocity. Such electron dispersion has been observed in the nightside (Kletzing and Torbert, 1994).

What is the spatial-temporal structure of the acceleration region? From the dispersion curve (low energy cut off of the downward electron changes 2 keV, 0.8 keV, and 0.4 keV in every 0.062 sec), one can obtain the time-of-flight distance $H_{TOF} = \Delta t{\cdot}\Delta(1/v_{e\|}) \sim 0.4 - 0.5$ Re, and the velocity-filter distance $H_{VF} = H_{TOF}{\cdot}(v_{sc}/v_c) \sim 10$ Re, where $v_{e\|}$, v_{sc} and v_c are velocities of the downward electron, satellite, and the convection along the satellite path.

The spread of the electron distribution in the energy domain indicates that the acceleration region is either a moving structure or a burst in a vertically spread region. The distance to the ultimate source (i.e., initial acceleration) is yet estimated the same as H_{TOF} even if the source (acceleration region) moves downward not faster than the downgoing electrons (another scenario is that the travelling Alfvén wave accelerate electrons as it propagates). Therefore, one can safely conclude that source of the time-dispersed electrons and subsequent STEB is within 1 Re above the ionosphere. In this case, the horizontal extent of the source should be at least 4 km along the satellite path.

Two obvious questions remain. The green-line auroral arcs are normally continuous in time and extended in longitude according to the past ground-based dayside observations (Sandholt et al., 1998; and references therein), and hence downward acceleration mechanism responsible for such aurora must be stable for at least several tens minutes. This does not agree with the short-lived nature of the electron burst in Figure 2.

Another problem is the meso-scale FAC direction during the observed electron burst because a downward FAC means upward net electron flux. Inside the FAC sheet (observed for several seconds), Freja could not detect such an upward electron signature, up to the highest detectable pitch angle (150°). One possible scenario is that a pre-existing FAC sheet causes a current-driven instability responsible for the observed electron burst, and this burst abruptly intensifies the continuous green aurora. In this case the amplitude of the AC magnetic field of the wave and the jump in DC magnetic field does not have to be linearly correlated. In fact, the amplitude of the wave field during Figure 2 event (1435:10 UT) is larger than that during the other electron burst at 1434:42 UT (Figure 3) while the latter shows a larger jump of the DC magnetic field (about 400 nT jump).

Figure 3

Fig. 3. Same as Figure 2 for at around 1434:40 UT. Minor signature in the upgoing direction (145° pitch angle) and coexisting downgoing FAC indicates that the electron burst is most likely bi-directional.

Before further discussion, let us examine the burst-like event at 1434:42 UT in Figure 3. This example (time-8) does not show visible time-of-flight dispersion. The burst is accompanied by a much stronger FAC than the previous case, and correspondingly it has the upward component as can be recognized by comparing $>$ 300 eV electrons between 30° and 150° pitch angles (the latter is inside the usual loss cone at Freja altitude). Considering the large jump in the magnetic field, Figure 3 observation suggests a bi-directional electron distribution although there is no measurement for pitch angles higher than 150°.

The large single step of ΔB_e near 1434:42 UT (it again takes a few seconds to complete the jump) indicates that the field structure is quasi-stationary. This type of magnetic field change, instead of bipolar dips, nor-

mally means a stationary conduction current instead of a short-lived flow burst or the geomagnetic field oscillation. To keep such stationary nature, the current carrier (upward electron component) must also be quasi-stationary. The coincidence between the largest step of DC magnetic field and strong electron burst is also reported by Potemra et al. (1987).

Thus both field and particle observations suggest that the long-lasting green auroral arc in the late morning BPS is better related to this event (Figure 3) than the previous case (Figure 2). If so, the source, i.e., the downward accelerated electron population, should also be quasi-stationary, including the burst-like electrons in Figure 3. Note that "quasi-stationary" includes the proposed scenario that a pre-existing steady FAC causes an instability which repeatedly forms "transient" downward electron bursts at the same location. Note also that the burst itself does not necessarily correspond to the auroral arc, but the potential acceleration (signature is seen before the burst at around 500 eV) could be the source of the aurora if such a potential structure is inherent to this "stationary" burst of Figure 3. In this case the green auroral arc and the FAC sheet match within 1 km distance.

Inversely, the electron dispersion in Figure 2 most likely originates from transient acceleration at 0.4-0.5 Re above the ionosphere, and is probably related to the transient aurora lying poleward of the stationary auroral arc. Thus, these two electron bursts are different in nature; the electron burst with clear dispersion in Figure 2 is probably related to the Alfvén wave and the transient aurora without strong FAC, whereas the electron burst at 1434:42 UT is probably associated with the majority of the large-scale FAC and the stable green arc. Past report (Chaston et al., 1999, and references therein) did not distinguish these differences. The energy of these bursts is sometimes as high as several keV.

2.2 Cusp

In the cusp and its vicinity, we again observe both types of electron bursts but with somewhat lower energy (a few hundred eV), as shown in Figure 4. There are many short-lived electron bursts similar to the BPS case, and each burst lasts at most 4 or 5 time steps (0.062 sec for each time step). Yet one can recognize, by comparing with Figure 2, the electron burst without clear dispersion (time-8). In addition, we found (not seen in Figure 4) injecting electrons with ordinary dispersion followed by STEB. Time-1 to time-3 may look like an inverted dispersion, but we believe it is not a real dispersion. It could simply be caused by temporal increase of acceleration energy. Some of the dispersionless burst could be a transient one injected from a very close source, but we cannot find out it due to the limit of the measurement resolution.

The AC electromagnetic disturbances inside the cusp

Figure 4

Fig. 4. Same as Figure 2 for at around 1440:30 UT.

proper are about the same level as those during the dispersive electron burst in BPS (Figure 2), and are more intense than those during the dispersionless electron burst in BPS (Figure 3). The DC magnetic disturbance associated with the electron burst is also about the same level as the Figure 2 case, but it is related only to the small-scale FACs that does not contribute to the large-scale cusp FACs (cf. Yamauchi et al., 2000).

Electrostatic acceleration signature for several hundred eV potential drop is also reported inside the cusp (Pfaff et al., 1998). This is again recognized in this orbit (Figure 4 of Yamauchi et al. (2000)). The 100-200 eV potential structure overlies the bursts in Figure 4. The potential value is different for different traversals. Due to the sensor threshold for electrons, such a potential structure can only be recognized when the potential drop is more than 100 eV. Yet we have identified such potential (> 150 eV) for more than 30 cusp traversals out of total 100 cusp traversals. The characteristic energy of this potential is generally lower than those in BPS (cf. Figure 1).

Unlike the BPS case, The electrostatic potential structure inside the cusp is not correlated with large- or meso-scale FAC. Therefore, we again reach the same conclusion as Yamauchi et al. (1998): the carrier of the large-scale cusp FAC is difficult to identify. The electrostatic potential without field-aligned current in the cusp is somewhat puzzling.

3 Summary of the Observations

We observed many different signatures of the low-energy electron population in the cusp and the dayside boundary layer: (1) downward electrons with transient acceleration signature, i.e., time dispersive super-Alfvénic electrons and subsequent super-thermal electron burst accompanied by a strong wave activity in both BPS and the cusp-cleft; (2) quasi-stationary electron burst in probably both upward and downward directions coinciding with a localized intense stationary FAC (large jump in ΔB_e) in BPS only; (3) less energetic downgoing electron burst without visible time dispersion in the cusp-cleft; (4) thermal electrons accelerated by an electrostatic potential structure in both BPS and the cusp-cleft. The first category, the transient acceleration, is associated with the Alfvén wave and is probably related to (and probably caused by) the pre-existing meso-scale FACs.

The first and the last types of acceleration are different between BPS and the cusp-cleft in their typical energy and flux, and these differences probably reflect the different auroral emissions in the cusp (red) and BPS (green). The second and third categories, electron bursts without visible dispersion, are also different in their forms. The second category has strong relation to localized FACs which accounts for most of the large-scale R-1 FAC, whereas the third category, common in the cusp, has only vague relation to meso-scale FACs, and have very little or no contribution to the large-scale (C-1, or C-0) FACs contrary to the BPS (R-1) case. C-1/C-0 FAC flows at the boundaries of the cusp only, whereas the electron acceleration (both bursty one and potential one) takes place in the entire cusp (Yamauchi et al., 2000).

The potential acceleration (of about a few hundred eV) is seen in the entire cusp regardless of the FAC directions. The potential acceleration is also seen in BPS, and its morphology is different between dawn and dusk, but this is out of the scope of this paper.

4 Discussion

We saw cusp traversals (e.g., orbit 6653) in which dispersive electron injections followed by STEB are mostly seen at the boundaries of the cusp whereas the cusp proper is mostly composed of electrostatically accelerated thermal electrons. The present case also showed potential acceleration signature in the cusp proper, but Figure 4 also showed the structured electrons in the cusp proper although the energy is lower in Figure 4 case than orbit 6653. It is not yet clear if one may distinguish the cusp and the cleft from these electron signatures.

Good coincidence between the dispersionless electrons in Figure 3 and the stationary FAC suggests that the bursty electrons are most likely bi-directional and quasi-stationary, and are responsible for the quasi-stationary green-line emission in BPS, which continues several tens minutes. This is not the case in the cusp-cleft. "Quasi-stationary" burst is probably maintained repeatedly by a current-driven instability.

The diffuse cusp red aurora during weak IMF (Sandholt, et al., 1998) can well be understood as caused by electrostatically accelerated electrons found throughout the cusp. The structured cusp red aurora during southward IMF is more controversy. Only a few strong arcs exist in the cusp-cleft region and they slowly move poleward (Sandholt et al., 1998, and references therein). Therefore, they must be caused by structured low-energy electrons which last at least several minutes. The only candidate in the satellite data is the dispersionless electron burst which carries a high flux of about 100 eV electrons. If so, it must be quasi-stationary.

No matter what is the case, the red aurora formation in the cusp is mostly attributed to the electron acceleration inside the magnetosphere but little to the direct entrance of the magnetosheath electrons without acceleration. The structures and dynamics of the cusp red aurora most likely reflect the acceleration mechanism above the ionosphere. Therefore, the poleward moving auroral forms in the cusp probably reflect the poleward propagation of the acceleration mechanism such as the Alfvén wave structure, but not the direct entrance of the magnetosheath electrons without acceleration, as cusp models by flux transfer event predict.

Acknowledgements. The Freja project is supported by Swedish National Space Board and German Space Agency.

References

Chaston, C.C., Carlson, C.W., Peria, W.J., et al. (1999) FAST observations of inertial Alfven waves in the dayside aurora, *Geophys. Res. Lett., 26*, 647.

Kletzing C.A., and Torbert, R.B. (1994) Electron time dispersion, *J. Geophys. Res., 99*, 2159.

Lundin, R., and Eliasson, L. (1991) Auroral energization process, *Ann. Geophys., 9*, 203.

Lysak, R.L. (1997) Propagation of Alfvén waves through the ionosphere, *Phys. Chem. Earth, 22*, 757.

Pfaff, R., Clemmons, J., Carlson, C.W., et al. (1998) Initial FAST observations of acceleration processes in the cusp, *Geophys. Res. Lett., 25*, 2037.

Potemra, T.A., Zanetti, L.J., Erlandson, R.E., et al. (1987) Observations of large-scale Birkeland currents with Viking, *Goephys. Res. Lett., 14*, 419.

Sandholt P.E., Farrugia, C.J., Moen, J., and Lybekk, B. (1998) The dayside aurora and its regulation by the interplanetary magnetic field, in *Polar Cap Boundary Phenomena*, edited by J. Moens, et al., Kluwer Acad. Pub., 189.

Winningham, J.D., Yasuhara, F., Akasofu, S.-I. and Heikkila, W.J. (1975) The latitudinal morphology of 10 eV to 10 keV electron fluxes during magnetically quiet and disturbed times in the 21:00-03.00 MLT sector, *J. Geophys. Res., 80*, 3138.

Yamauchi, M., Lundin, R., and Potemra, T. (1995) Dynamic response of the cusp morphology to the IMF changes: An example observed by Viking, *J. Geophys. Res., 100*, 7661.

Yamauchi, M., Lundin, R., Eliasson, L., et al. (1998) Relationship between large-, meso, and small-scale field-aligned currents and their current carriers, in *Polar Cap Boundary Phenomena*, edited by J. Moens, et al., Kluwer Acad. Pub., 173.

Yamauchi, M., Lundin, R., Eliasson, L., et al. (2000) Independency of the dayside field-aligned current system: A restriction to cusp models, in *Magnetospheric Current Systems*, edited by Fujii et al., Geophysical Monograph *118*, AGU, 245.